

Direct Visualization of Protein Association in Living Cells with Complex-Edited Electron Microscopy**

Rachel J. Dexter and Alanna Schepartz*

Dedicated to Ronald Breslow on the occasion of his 80th birthday

Interactions between and among proteins regulate most cell functions, yet detecting these interactions in living cells, especially at high resolution, remains a challenge. Protein complementation,^[1] proximity-induced biotinylation,^[2] FRET (Förster resonance energy transfer),^[3] and bipartite tetracysteine display^[4] can all detect interactions between proteins, but only at the moderate resolution provided by epifluorescent microscopy (approximately 200 nm). Super-resolution imaging has begun to overcome this diffraction limit,^[5] but it cannot detect protein complexes at the near-atomic-level resolution achievable using electron microscopy (EM).^[6] Individual tetracysteine-containing proteins can be visualized using EM by use of the biarsenical dye 4,5-bis(1,3,2-dithiarsolan-2-yl)resorufin (ReAsH).^[7–9] Irradiation of a protein–ReAsH complex at 585 nm in the presence of oxygen and 3,3'-diaminobenzidine (DAB) catalyzes the formation of an osmophilic DAB polymer that is opaque to electron beams and appears in the electron microscope as a fine granular precipitate.^[7–9] An analogous method able to identify a discrete protein complex within a living cell, followed by fixation and sectioning as required by EM, would provide a powerful tool for visualizing at high resolution the interactions between proteins in their native environments.

Recently we reported that ReAsH could be used in solution to visualize discrete protein complexes provided that each member of the protein assembly contributes a single CysCys motif to recapitulate an appropriate, albeit bipartite, tetracysteine binding site for ReAsH.^[4] Subsequently we explored the structure and flexibility requirements of bipartite tetracysteine display,^[10] and described its application to generate a prototype for a fluorescent-protein-free Src kinase sensor.^[11] Others have used bipartite tetracysteine display to monitor conformational states of cellular retinoic acid binding protein (CRAB-P) in *E. coli*.^[12] Here we describe a new method—complex-edited electron microscopy (CE-EM, Figure 1)—that combines bipartite tetracysteine display^[4]

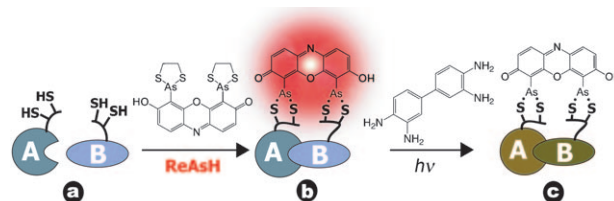


Figure 1. Complex-edited electron microscopy (CE-EM). a) Each member of the protein complex is modified by addition of a single CysCys motif that facilitates selective labeling of the complex with ReAsH (b). Irradiation of the ReAsH complex in the presence of diaminobenzidine (DAB) polymerizes the DAB surrounding each protein complex; the characteristic brown precipitate forms. c) Subsequent treatment with OsO_4 permits selective visualization of protein complexes by EM.

with electron microscopy. CE-EM facilitates the direct and selective labeling of a discrete protein complex in a living cell, followed by imaging with the extraordinary resolution of electron microscopy. CE-EM represents a unique tool for selectively visualizing a protein–protein complex in a living cell with the near-atomic resolution achievable using electron microscopy.

In our initial description of bipartite tetracysteine display^[4] we reported that ReAsH could be used to differentiate a wildtype (wt) GCN4–eGFP coiled-coil fusion protein from a variant containing a single destabilizing substitution (L_{20}P) in living HeLa cells. We chose to build upon these results to evaluate the feasibility of CE-EM. HeLa cells were transiently transfected with DNA encoding an analogous variant of each protein used previously^[4] that contained a nuclear localization signal (NLS) PKKKRKVEDA^[13] fused to the eGFP C terminus (C_2 -GCN4-NLS and C_2 - L_{20}P -NLS, respectively, Figure 2). Additional variants included eGFP fused to an optimized sequence for ReAsH binding (FLNCCPGCCMEP) (C_4 -Opt-NLS) as a positive control, and eGFP fused to wt GCN4 lacking a Cys–Cys sequence (A_2 -GCN4-NLS) as a negative control. HeLa cells transiently expressing each fusion protein were treated with ReAsH, washed, and visualized using epifluorescent microscopy (Figure 2). As expected, the nuclei of cells expressing any of the four fusion proteins showed fluorescence at the eGFP emission maximum (488 nm), demonstrating that each fusion protein was expressed and properly localized in living cells. Nuclear localization was confirmed by treating the HeLa cells with Hoechst 33342, a DNA intercalator^[14] (Supporting Information, Figure S1). In contrast, only the nuclei of those cells expressing C_4 -Opt-NLS and C_2 -GCN4-NLS were fluo-

[*] Dr. R. J. Dexter, Prof. A. Schepartz
Department of Chemistry, Yale University
New Haven, CT 06510 (USA)
Fax: (+1) 203-432-3486
E-mail: alanna.schepartz@yale.edu
Homepage: <http://www.schepartzlab.yale.edu>

[**] This work was supported by the NIH (GM 83257). We are grateful to the Yale Center for Cellular and Molecular Imaging for assistance with electron microscopy.

Supporting information for this article is available on the WWW under <http://dx.doi.org/10.1002/anie.201003217>.

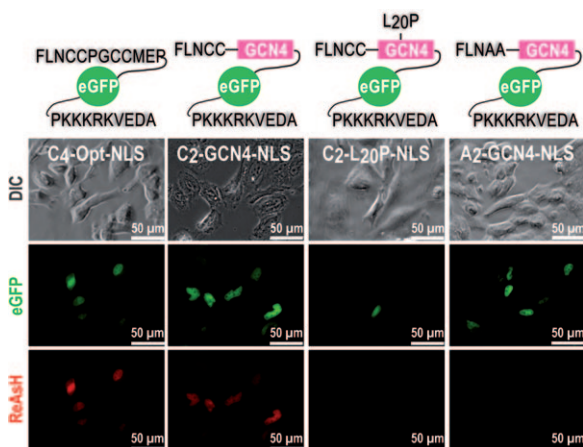


Figure 2. ReAsH binding/fluorescence of nuclear-localized GCN4 constructs in living cells. Cells expressing each of the four fusion proteins shown were treated with ReAsH (180 nM, 3 h), washed with British Anti-lewisite (BAL; 250 μ M, 20 min), and visualized on a Zeiss Axiovert 200 M microscope equipped with an X-Cite 120 short arc xenon lamp. Differential interference contrast (DIC) images in the top row show total cells in the field of view; the second row shows the subcellular location of fluorescence due to eGFP (green, $\lambda_{\text{ex}} = 470 \pm 40$ nm, $\lambda_{\text{em}} = 540 \pm 50$ nm) and detects fusion protein expression; the third row shows the subcellular location of fluorescence due to ReAsH (red, $\lambda_{\text{ex}} = 545 \pm 12$ nm, $\lambda_{\text{em}} = 605 \pm 35$ nm). These images verify that, when expressed in HeLa cells, C₄-Opt-NLS, C₂-GCN4-NLS, C₂-L₂₀P-NLS, and A₂-GCN4-NLS localize to nuclei, as expected, but only C₄-Opt-NLS and C₂-GCN4-NLS bind ReAsH.

resent at the ReAsH emission maximum (608 nm). No fluorescence due to ReAsH was evident in cells expressing C₂-L₂₀P-NLS and A₂-GCN4-NLS, which either dimerize poorly (C₂-L₂₀P-NLS) or lack a functional ReAsH binding site (A₂-GCN4-NLS). We conclude that C₂-GCN4-NLS assembles in HeLa cell nuclei into a coiled-coil dimer that effectively recapitulates a binding site for ReAsH. While the C₂-L₂₀P-NLS and A₂-GCN4-NLS proteins are expressed, they either do not associate (C₂-L₂₀P-NLS) or cannot bind ReAsH (A₂-GCN4-NLS) and no ReAsH fluorescence is observed.

To evaluate if bipartite tetracysteine display would support the visualization of a dimeric protein assembly using EM, the cells were fixed, treated with a standard cocktail to inhibit mitochondrial respiration,^[8,15] incubated with DAB, and illuminated at 545 ± 24 nm. No DAB polymerization was observed by epifluorescent microscopy when cells expressing C₄-Opt-NLS were illuminated in the absence of DAB, even after 2 h (Figure S2). When cells expressing C₄-Opt-NLS were illuminated in the presence of DAB, the disappearance of ReAsH emission (608 nm) was concomitant with the formation of a brownish precipitate within 1 h (Figure 3). A high level of DAB polymerization also appeared in the nuclei of cells expressing C₂-GCN4-NLS, but not in those expressing the dimerization-impaired variant C₂-L₂₀P-NLS or one that lacked a ReAsH binding site, A₂-GCN4-NLS. At longer illumination times (2 h), polymerization is apparent throughout the cytosol and nuclei of cells expressing C₄-Opt-NLS and C₂-GCN4-NLS (Figure S2). Minimal polymerization is seen in any region of cells expressing C₂-L₂₀P-NLS or A₂-GCN4-NLS, even after 2 h of illumination. We note that although

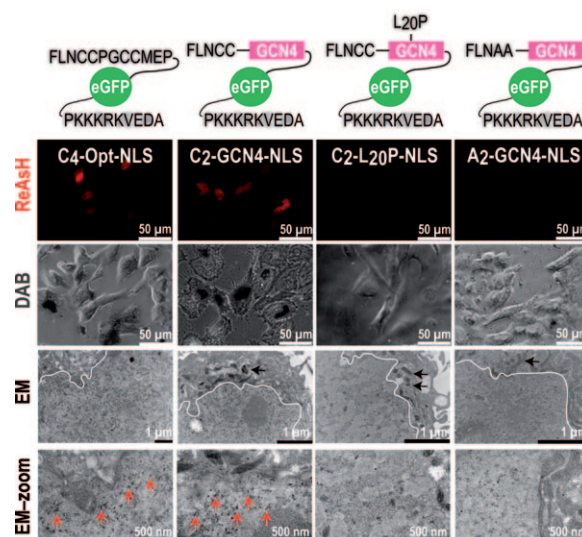


Figure 3. Electron microscopy of cells expressing C₄-Opt-NLS, C₂-GCN4-NLS, C₂-L₂₀P-NLS, and A₂-GCN4-NLS after treatment with ReAsH, DAB, *hν*, and OsO₄. Cells expressing each of the four fusion proteins were treated with ReAsH as described in the legend to Figure 2. Epifluorescent images monitoring emission at the ReAsH maximum (red, $\lambda_{\text{ex}} = 545 \pm 12$ nm, $\lambda_{\text{em}} = 605 \pm 35$ nm) are repeated for clarity (top row). DAB polymerization is visible only in the nuclei of cells expressing C₄-Opt-NLS or C₂-GCN4-NLS (row 2). Electron micrographs of cells at low (row 3, scale bar = 1 μ m) and high (row 4, scale bar = 500 nm) magnification are shown. The nuclear membrane in each low resolution image is identified by a white line. Examples of mitochondrial staining are identified by black arrows. Examples of areas within the nuclei that show increased electron density are identified by red arrows.

GFP has been used to photo-oxidize DAB,^[16] (albeit inefficiently)^[17] the absence of DAB polymerization in the nuclei of cells expressing C₂-L₂₀P-NLS and A₂-GCN4-NLS is definitive evidence that DAB polymerization in cells expressing C₂-GCN4-NLS requires bound ReAsH. Cells were then treated with osmium tetroxide (1% OsO₄, 1 h) and prepared for EM.

The EM images shown in Figure 3 display a level of electron density that parallels the extent of DAB polymerization visible by epifluorescent microscopy. All EM images clearly demonstrate an articulated nuclear membrane (dotted white line; see also Figure S3). However, only those cells expressing C₄-Opt-NLS or C₂-GCN4-NLS show increased electron density within their nuclei, with no increased density in the nucleolus. No increase in electron density is observed in the nuclei of cells expressing C₂-L₂₀P-NLS, A₂-GCN4-NLS (Figure 3) or in cells expressing C₄-Opt-NLS that were not treated with ReAsH or DAB (Figure S3). The increased electron density seen sporadically in the mitochondria is likely due to insufficient inhibition of cellular respiration before polymerization of DAB. Comparison of the images obtained using CE-EM (Figure 3) with those obtained after staining with rabbit anti-GFP/protein A gold (Figure S4) demonstrate that the sensitivity of CE-EM is at least as high as that obtainable by traditional methods, with the added advantage that the CE-EM technique requires protein-protein complex formation and occurs in living cells.

To quantify the differences in electron density among the four cell populations, we analyzed the images using Image J.^[18] Multiple square areas (400 × 400 pixels) from each nuclei were individually masked, and the total area of increased electron density (A_{ED}) within each was calculated and averaged (Figure S3). The value of A_{ED} in the nuclei of cells expressing C₄-Opt-NLS and C₂-GCN4-NLS is over four times greater than in analogous cells that were not treated with ReAsH, and more than twice of that in ReAsH-treated cells expressing C₂-L₂₀P-NLS and A₂-GCN4-NLS. These comparative A_{ED} values provide a quantitative assessment of what is clearly visible in Figure 3: the GCN4 homodimer can be selectively visualized in the nucleus using complex-edited electron microscopy.

In summary, we describe a technique, complex-edited electron microscopy, which facilitates the direct and selective visualization of discrete protein–protein complexes at high resolution using electron microscopy. Notably, the molecular event that initiates this visualization—reaction of a protein–protein complex with ReAsH—occurs in living cells.

Received: May 27, 2010

Published online: ■ ■ ■ ■, 2010

Keywords: bipartite tetracysteine display · electron microscopy · protein–protein interactions · ReAsH · site-specific labeling

- [1] a) K. M. Arndt, J. N. Pelletier, K. M. Muller, T. Alber, S. W. Michnick, A. Pluckthun, *J. Mol. Biol.* **2000**, *295*, 627–639; b) A. Galarneau, M. Primeau, L. E. Trudeau, S. W. Michnick, *Nat. Biotechnol.* **2002**, *20*, 619–622; c) C. D. Hu, Y. Chinenov, T. K. Kerppola, *Mol. Cell* **2002**, *9*, 789–798; d) C. D. Hu, T. K. Kerppola, *Nat. Biotechnol.* **2003**, *21*, 539–545; e) T. K. Kerppola, *Chem. Soc. Rev.* **2009**, *38*, 2876–2886; f) K. E. Luker, M. C. P. Smith, G. D. Luker, S. T. Gammon, H. Piwnica-Worms, D. P. Piwnica-Worms, *Proc. Natl. Acad. Sci. USA* **2004**, *101*, 12288–12293; g) B. Nyfeler, S. W. Michnick, H. P. Hauri, *Proc. Natl. Acad. Sci. USA* **2005**, *102*, 6350–6355; h) J. N. Pelletier, K. M. Arndt, A. Pluckthun, S. W. Michnick, *Nat. Biotechnol.* **1999**, *17*, 683–690; i) J. N. Pelletier, F. X. Campbell-Valois, S. W. Michnick, *Proc. Natl. Acad. Sci. USA* **1998**, *95*, 12141–12146; j) I. Remy, F. X. Campbell-Valois, S. W. Michnick, *Nat. Protoc.* **2007**, *2*, 2120–2125; k) I. Remy, G. Ghaddar, S. W. Michnick, *Nat. Protoc.* **2007**, *2*, 2302–2306.
- [2] M. Fernandez-Suarez, T. S. Chen, A. Y. Ting, *J. Am. Chem. Soc.* **2008**, *130*, 9251–9253.
- [3] a) J. Llopis, S. Westin, M. Ricote, J. H. Wang, C. Y. Cho, R. Kurokawa, T. M. Mullen, D. W. Rose, M. G. Rosenfeld, R. Y. Tsien, C. K. Glass, *Proc. Natl. Acad. Sci. USA* **2000**, *97*, 4363–4368; b) N. P. Mahajan, K. Linder, G. Berry, G. W. Gordon, R. Heim, B. Herman, *Nat. Biotechnol.* **1998**, *16*, 547–552; c) A. Miyawaki, J. Llopis, R. Heim, J. M. McCaffery, J. A. Adams, M. Ikura, R. Y. Tsien, *Nature* **1997**, *388*, 882–887; d) A. Miyawaki, *Dev. Cell* **2003**, *4*, 295–305; e) J. van der Wal, R. Habets, P. Varnai, T. Balla, K. Jalink, *J. Biol. Chem.* **2001**, *276*, 15337–15344; f) Z. P. Xia, Q. Zhou, J. L. Lin, Y. C. Liu, *J. Biol. Chem.* **2001**, *276*, 1766–1771.
- [4] N. W. Luedtke, R. J. Dexter, D. B. Fried, A. Schepartz, *Nat. Chem. Biol.* **2007**, *3*, 779–784.
- [5] B. Huang, M. Bates, X. Zhuang, *Annu. Rev. Biochem.* **2009**, *78*, 993–1016.
- [6] a) K. Cortese, A. Diaspro, C. Tacchetti, *J. Histochem. Cytochem.* **2009**, *57*, 1103–1112; b) S. A. Muller, U. Aebi, A. Engel, *J. Struct. Biol.* **2008**, *163*, 235–245.
- [7] G. Gaietta, T. J. Deerinck, S. R. Adams, J. Bouwer, O. Tour, D. W. Laird, G. E. Sosinsky, R. Y. Tsien, M. H. Ellisman, *Science* **2002**, *296*, 503–507.
- [8] G. M. Gaietta, B. N. G. Giepmans, T. J. Deerinck, W. B. Smith, L. Ngan, J. Llopis, S. R. Adams, R. Y. Tsien, M. H. Ellisman, *Proc. Natl. Acad. Sci. USA* **2006**, *103*, 17777–17782.
- [9] J. Lanman, J. Crum, T. J. Deerinck, G. M. Gaietta, A. Schneemann, G. E. Sosinsky, M. H. Ellisman, J. E. Johnson, *J. Struct. Biol.* **2008**, *161*, 439–446.
- [10] J. L. Goodman, D. B. Fried, A. Schepartz, *ChemBioChem* **2009**, *10*, 1644–1647.
- [11] S. Ray-Saha, A. Schepartz, *ChemBioChem* **2010**, DOI: 10.1002/cbic.201000234.
- [12] B. Krishnan, L. M. Gierasch, *Chem. Biol.* **2008**, *15*, 1104–1115.
- [13] J. P. S. Makkerh, C. Dingwall, R. A. Laskey, *Curr. Biol.* **1996**, *6*, 1025–1027.
- [14] J. W. Ellwart, P. Dormer, *Cytometry* **1990**, *11*, 239–243.
- [15] C. Meisslitzer-Ruppitsch, C. Rohrl, J. Neumuller, M. Pavelka, A. Ellinger, *J. Microsc.* **2009**, *235*, 322–335.
- [16] a) M. Grabenbauer, W. J. C. Geerts, J. Fernandez-Rodriguez, A. Hoenger, A. J. Koster, T. Nilsson, *Nat. Methods* **2005**, *2*, 857–862; b) C. Meisslitzer-Ruppitsch, M. Vetterlein, H. Stangl, S. Maier, J. Neumuller, M. Freissmuth, M. Pavelka, A. Ellinger, *Histochem. Cell Biol.* **2008**, *130*, 407–419.
- [17] A. Jimenez-Banzo, S. Nonell, J. Hofkens, C. Flors, *Biophys. J.* **2008**, *94*, 168–172.
- [18] T. J. Collins, *Biotechniques* **2007**, *43*, S25–S30.

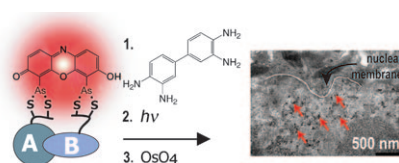
Communications



Protein Imaging

R. J. Dexter, A. Schepartz* — ■■■■-■■■■

Direct Visualization of Protein Association in Living Cells with Complex-Edited Electron Microscopy



Good partnership: A novel technique called complex-edited electron microscopy (CE-EM) combines bipartite tetra-cysteine display with EM and permits high-resolution imaging of discrete protein complexes (A and B in the picture). The strategy facilitates the direct and selective labeling of discrete protein complexes in living cells, followed by imaging with the extraordinary resolution of EM.